JCTC Journal of Chemical Theory and Computation

Backbone Importance for Protein−Protein Binding†

Irina S. Moreira, Pedro A. Fernandes, and Maria J. Ramos*

REQUIMTE/Departamento de Química, Faculdade de Ciências da Universidade do Porto, Rua do Campo Alegre 687, 4169-007 Porto, Portugal

Received December 28, 2006

Abstract: Although a number of studies have focused on the physical and chemical properties of protein−protein interfaces of complexes to determine their unique features, the importance of the backbone hydrogen bonds to protein−protein binding has been neglected due to the difficulty of quantitatively measuring their contribution to the free binding energy. In this study we are presenting a computational approach that allows the estimation of the contribution to the free binding energy of the CO and NH groups of the backbone of various proteic complexes. A correlation between the quantitative calculated free binding energy contribution of the CO and NH backbone groups of the interfacial residues and the qualitative values expected for this kind of interaction was achieved. The contribution of the backbone to the $\Delta\Delta G_{binding}$ is significant. The average $\Delta\Delta G_{binding}$ contribution of the intermolecular hydrogen bonds of the backbone is 1.77 kcal/mol, which is very similar to the average contribution of the different side chains to the $\Delta\Delta G_{binding}$, with a value of 1.75 kcal/mol. Therefore, the application of this computational approach as well as an alanine scanning mutagenesis study is essential to a more detailed comprehensive knowledge of proteic complex formation.

Introduction

Crystallographic structures of proteins cocrystallized with various ligands, together with structural and thermodynamic studies, made possible the identification of the structural binding epitopes (amino acid residues which are in contact with the other binding partner).[1−3] These studies have been completed with experimental and computational alanine-scanning mutagenesis of protein−protein interfacial residues that allowed the definition of the functional binding epitopes (contact residues that make energetic contributions to binding).[4−7]

Although a number of studies have focused on the physical and chemical properties of protein−protein interfaces of complexes to determine their unique features, the importance of the backbone hydrogen bonds to protein−protein binding has been neglected due to the difficulty of quantitatively measuring their contribution to the free binding energy.[8,9] Protein backbone is an important contributor to interfaces because it represents in average of about one-fifth of the interface area. These hydrogen bonds contribute significantly to the stability of a protein structure, because they are the major contributors to the electrostatic interactions between proteins.[10] However, hydrogen bonds are extremely important not only for stability but also because they affect other physicochemical properties of a molecule such as solubility, partitioning, distribution, permeability, and specificity that are crucial for drug development.[11] Hydrogen bonds are essential in determining binding specificity because they contribute favorably to the free energy of binding, but unfulfilled hydrogen bonds donor/acceptor could substantially destabilize the binding. Such a contrast in energetics contributes to a high selectivity in matching the hydrogen bonds between proteins and confers binding specificity.

The hydrogen bond is viewed as an interaction that has covalent, electrostatic, and van der Waals character and an energy that ranges from 0.25 to roughly 40 kcal/mol. The atoms involved in the hydrogen bond determine the strength of this electrostatic interaction, with the hydrogen bonds that contribute more to the binding normally made between atoms buried in the interior of the protein.[6] Intermolecular hydrogen

† Dedicated to Professor Dennis R. Salahub on the occasion of his 60th birthday.

* Corresponding author e-mail: mjramos@fc.up.pt.

10.1021/ct6003824 CCC: $37.00
Published on Web 04/04/2007

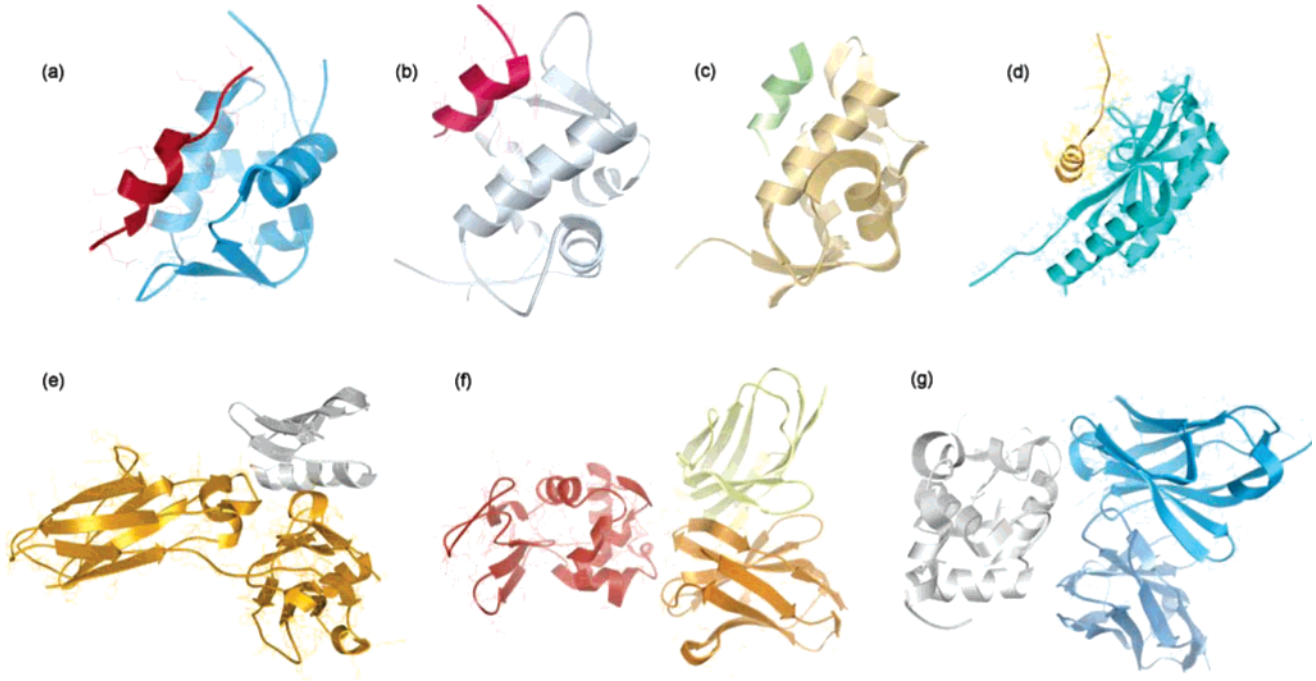

Figure 1. Molecular representation of the complexes formed between (a) the hMDM2 and the P53 protein (1YCR); (b) the xMDM2 and the P53 protein (1YCQ); (c) the hMDM2 and an optimized P53 protein (1T4F); (d) a cell division protein ZipA and a cell division protein FtsZ (1F47); (e) a human immunoglobulin IgG complexed with the C2 fragment of streptococcal protein G (1FCC); (f) the lysozyme HEL and the antibody FvD1.3 (1VFB); and (g) the hen egg-white lysozyme (HEL) and the antibody HyHEL-10 (1C08).

Scheme 1. Thermodynamic Cycle Used To Calculate the Complexation Free Energy

$$\begin{array}{ccc} \text{ligand}_{aq} + \text{receptor}_{aq} & \xrightarrow{\Delta G_{bind}} & \text{complex}_{aq} \\ -\Delta G^{lig}_{solv} \downarrow \quad -\Delta G^{rec}_{solv} \downarrow & & \uparrow +\Delta G^{cpx}_{solv} \\ \text{ligand}_{gas} + \text{receptor}_{gas} & \xrightarrow{\Delta G_{gas}} & \text{complex}_{gas} \end{array}$$

bonds are generally weaker and have a larger diversity than the intramolecular ones. The lower quality of the interface hydrogen bond interactions can be attributed to the more hydrophilic side chains buried in the binding protein−protein interface than in the folded monomer interior.[11]

Besides being very important from a conceptual point of view, understanding the role of the protein backbone is fundamental to understand, control, and manipulate protein complexes. As these complexes are involved in countless biological processes it is important for rational drug design to measure not only the contribution of the amino acid side chains but also the contribution of the protein backbone. Therefore, we have developed a computational method that allows the measurement of the free binding energy contribution of the different NH and CO atoms. This method was applied to seven protein−protein complexes that have a diverse molecular profile possessing a variety of functions and sizes.

Materials and Methods

1. Model Setup. The starting crystallographic structures for the simulations were the complexes formed between the hMDM2 and the P53 protein,[12] between the xMDM2 and the P53 protein,[12] between the hMDM2 and an optimized P53 protein,[13] between a cell division protein ZipA and a cell division protein FtsZ,[14] between a human immunoglobulin IgG complexed with the C2 fragment of streptococcal protein G,[15] between the lysozyme HEL and the antibody FvD1.3,[16] and between the hen egg-white lysozyme (HEL) and the antibody HyHEL-10[17] (all represented in Figure 1). They were taken from the RCSB Protein Data Bank with PDB entries 1YCR, 1YCQ, 1T4F, 1F47, 1FCC, 1VFB, and 1C08 and with resolutions of 2.60 Å, 2.30 Å, 1.90 Å, 1.95 Å, 3.50 Å, 1.80 Å, and 2.30 Å, respectively. The systems comprised a total of 98, 99, 97, 159, 262, 352, and 350 amino acid residues. All residues were included in their physiological protonation states (charged Glu, Asp, Lys, and Arg, all other residues neutral). In the molecular simulations the solvent was modeled through a modified Generalized Born solvation model[18] being the structure first minimized with 1000 steps of steepest decent followed by 1000 steps of conjugated gradient to release the bad contacts in the crystallographic structure. Subsequently, molecular dynamics (MD) simulations of 5, 4, 4, 4, 5, 3, and 3 ns, respectively, were performed starting from the minimized structure. All molecular mechanics simulations presented in this work were carried out using the sander module, implemented in the Amber8[19] simulations package, with the *Cornell* force field.[20] Bond lengths involving hydrogens were constrained using the SHAKE algorithm,[21] and the equations of motion were integrated with a 2 fs time-step being the nonbonded interactions truncated with a 16 Å cutoff. The temperature of the system was regulated by the Langevin thermostat.[22−24]

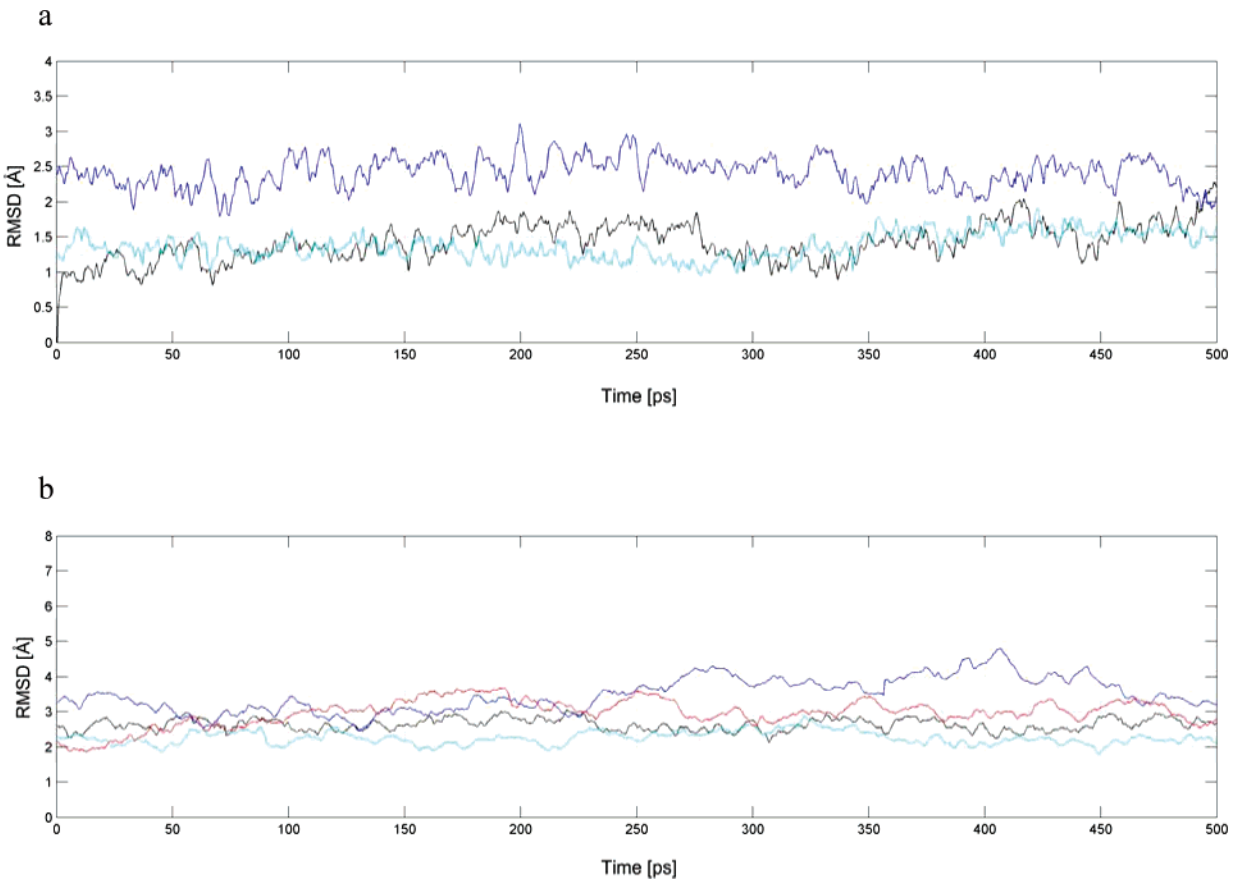

Figure 2. rmsd plots for the protein backbone of the complex formed between (a) (in black) the hMDM2 and the P53 protein (1YCR); (in blue) the xMDM2 and the P53 protein (1YCQ); and (in cyan) the hMDM2 and an optimized P53 protein (1T4F) and (b) (in black) a cell division protein ZipA and a cell division protein FtsZ (1F47); (in blue) a human immunoglobulin IgG complexed with the C2 fragment of streptococcal protein G (1FCC); (in cyan) the lysozyme HEL and the antibody FvD1.3 (1VFB); and (in red) the antibody HyHEL-10 (1C08) relative to its initial structure.

In force field Hamiltonians hydrogen bonds are due primarily to partial electrostatic charges, and therefore the energetic is determined by the values of the partial charges. To understand the importance of the backbone hydrogen bonds we have measured the free binding differences generated upon deletion of the charge of the amide (NH) and carbonyl (CO) groups. To ensure electroneutrality we have distributed the remaining partial charge proportionally by the remaining atoms of the corresponding residue. This procedure was made taking into account the proportions of the different atoms to the final charge of the amino-acid residue. For the binding free energy calculations, 25 snapshots of the complexes were extracted every 20 ps for the last 500 ps of the run.

2. Hydrogen Bonds at the Backbone of the Interfacial Residues. The complexation free energy can be calculated using the thermodynamic cycle shown in Scheme 1 where ΔG_{gas} is the interaction free energy between the ligand and the receptor in the gas phase. ΔG_{solv}^{lig}, ΔG_{solv}^{rec}, and ΔG_{solv}^{cpx} are the solvation free energies of the ligand, the receptor, and the complex, respectively. The binding free energy difference between the mutant (complex generated upon deletion of the amide and carbonyl groups) and wild type complexes is defined as

$$\Delta\Delta G_{binding} = \Delta G_{binding-mutant} - \Delta G_{binding-wild\ type} \quad (1)$$

The binding free energy of two molecules is the difference between the free energy of the complex and the respective monomers (the receptor and the ligand).

$$\Delta G_{binding-molecule} = G_{complex} - (G_{receptor} + G_{ligand}) \quad (2)$$

The free energy of the complex and respective monomers can be calculated by summing the internal energy (bond, angle, and dihedral), the electrostatic and the van der Waals interactions, the free energy of polar solvation, the free energy of nonpolar solvation, and the entropic contribution for the molecule free energy:

$$G_{molecule} = E_{internal} + E_{electrostatic} + E_{vdw} + G_{polar\ solvation} + G_{nonpolar\ solvation} - TS \quad (3)$$

The first three terms were calculated using the *Cornell* force field[20] with no cutoff. The electrostatic solvation free energy was calculated by solving the Poisson−Boltzmann equation with the software Delphi v.4,[25,26] using the same methodology of previous works which has been shown in an earlier work to constitute a good compromise between accuracy and computing time.[27] Albeit the use of an internal dielectric value of 2 or 4 did not influence the results significantly, for the energy calculations we have used an internal dielectric constant value of 3 due to the polar nature of the groups in question. The nonpolar contribution to

Table 1. Results of the Study of the Free Binding Energy Contribution of the Different NH and CO Atoms[a]

PDB files	protein	residue	$\Delta\Delta G_{binding}$	PDB files	protein	residue	$\Delta\Delta G_{binding}$
1YCR	P53	Thr18	−0.27	1YCR	P53	Trp23	−1.29
		Phe19	−0.29			His24	−0.47
		Ser20	0.26			Leu25	−0.84
		Asp21	−0.05			Leu26	−0.16
		Leu22	0.09				
1YCR	hMDM2	**Leu54**	**1.27**	1YCR	hMDM2	Tyr67	0.08
		Leu57	−0.01			Gln72	−1.12
		Ile61	0.09			Val93	−0.31
		Met62	0.10			Ile99	0.28
1YCQ	P53	Thr18	−0.52	1YCQ	P53	Trp23	−0.28
		Phe19	−0.35			His24	−0.18
		Ser20	−0.1			Leu25	0.20
		Asp21	−0.15			Leu26	0.34
		Leu22	−0.12				
1YCQ	xMDM2	**Ile50**	**1.62**	1YCQ	xMDM2	Tyr63	0.15
		Leu53	0.05			Gln68	−1.40
		Ile57	0.36			Val89	−0.49
		Met58	0.27			His90	0.16
1T4F	P53	Phe19	−0.37	1T4F	P53	Tyr22	−0.51
		Met20	−0.11			Trp23	−1.50
		Asp21	−0.27			Glu24	−0.44
1T4F	xMDM2	Leu54	0.15	1T4F	xMDM2	Tyr67	0.04
		Leu57	0.15			Gln72	−0.72
		Ile61	**0.41**			Val93	−0.48
		Met62	**0.30**			Ile99	−0.05
1F47	FtsZ	Asp370	−0.22	1F47	FtsZ	Phe377	0.23
		Tyr371	0.49			Leu378	−0.06
		Leu372	−0.43			Arg379	0.21
		Asp373	−1.66			Lys380	−0.14
		Ile374	**1.75**				
1F47	ZipA	Val194	0.15	1F47	ZipA	Lys250	−0.26
		Ile196	0.06			Thr253	−0.05
		Asp225	−0.09			Thr267	0.37
		Met226	−0.14			Ile268	0.01
		Ile228	0.12			Phe269	0.04
		Asn247	−1.08			Met270	−0.01
		Met248	−0.38			Gln271	0.01
		Val249	−1.48				
1FCC	protein G (C2 fragment)	Thr25	−0.28	1FCC	protein G (C2 fragment)	Asp40	0.85
		Glu27	1.36			Glu42	0.07
		Lys28	−0.18			Trp43	−0.44
		Lys31	0.22			Thr44	0.29
		Asn35	−0.51			Tyr45	−0.14
1FCC	IgG1	**Ile253**	**2.98**	1FCC	IgG1	Asn434	−1.48
		Ser254	**5.07**			His435	−0.84
		Glu380	0.28			Tyr436	−0.70
		Ser426	0.07			Thr437	0.02
		Met428	0.01			Gln438	−0.09
		His433	−0.58				
1VFB	antibody FvD1.3 VL	His30	−0.13	1VFB	antibody FvD1.3 VL	Thr53	−0.10
		Tyr32	−0.25			Trp92	−1.20
		Tyr49	−0.26			Ser93	−0.48
		Tyr50	−0.65				
1VFB	antibody FvD1.3 VH	Thr30	0.27	1VFB	antibody FvD1.3 VH	Glu98	0.59
		Tyr32	−0.35			Arg99	−0.13
		Trp52	0.09			Asp100	−0.73
		Asn56	0.20			Tyr101	−0.49
		Asp58	−0.05				
1VFB	HEL	Asp18	0.82	1VFB	HEL	Asp119	0.02
		Asn19	−0.1			Val120	0.8
		Tyr23	0.66			Gln121	0.41
		Ser24	**3.69**			Ile124	−0.15
		Lys116	−1.42			Arg125	−0.54
		Thr118	−0.81			Leu129	−0.13
1C08	HyHEL-10 VL	Asn31Ala	0.13	1C08	HyHEL-10 VL	Asp32Ala	−0.57
		Asn32ala	−0.18			Tyr50Ala	−0.41
		Tyr50Ala	−0.06			Tyr53Ala	−0.32
		Gln53Ala	−0.34			Tyr58Ala	−0.07
		Tyr96Ala	−0.45			Asp101Ala	−0.01
1C08	HEL	His15Ala	0.36	1C08	HEL	Asn93Ala	0.12
		Tyr20Ala	−0.50			Lys96Ala	−0.40
		Arg21Ala	0.08			Lys97Ala	−1.76
		Trp63Ala	0.17			Ile98Ala	0.84
		Arg73Ala	−0.62			Ser100Ala	−0.45
		Leu75Ala	0.29			Asp101Ala	0.20
		Thr89Ala	−0.22				

[a] All the energies are in kcal/mol.

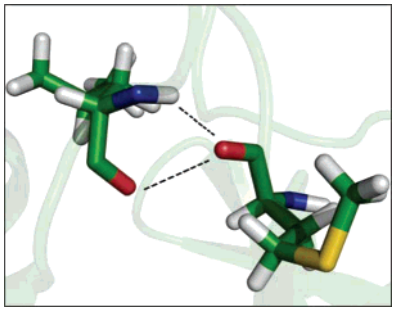

Figure 3. Molecular representation of the interactions established between the Met248 of the ZipA protein and the Leu372 of the binding partner in the 1F47 complex.

solvation free energy due to van der Waals interactions between the solute and the solvent and cavity formation was modeled as a term that is dependent on the solvent accessible surface area of the molecule. It was estimated using an empirical relation, $\Delta G_{\text{nonpolar}} = \sigma A + \beta$, where A is the solvent-accessible surface area that was estimated using the Molsurf program, which is based on the idea primarily developed by Michael Connolly.[28] σ and β are empirical constants, and the values used were 0.00542 kcal Å^{-2} mol^{-1} and 0.92 kcal mol^{-1}, respectively. The entropy term, obtained as the sum of translational, rotational, and vibrational components, was not calculated, because it was assumed that its contribution to $\Delta\Delta G_{\text{binding}}$ is negligible.[29]

Results

To obtain reliable estimates of the relative binding energy it was important to ensure that equilibration was achieved. In Figure 2a,b we have plotted the root-mean-square deviations (rmsd) for the backbone atoms of the seven complexes (1YCR, 1YCQ, 1T4F, 1F47, 1FCC, 1VFB, and 1C08) for the production MD simulation (the last 500 ps). As we can see the MD simulations are very stable with rmsd values lower than 2.0, 3.0, 2.0, 3.0, 4.0, 2.5, and 3.5 for the complexes 1YCR, 1YCQ, 1T4F, 1F47, 1FCC, 1VFB, and 1C08, respectively.

Table 1 summarizes the results of the study of the free binding energy contribution of the different NH and CO atoms applied to the seven complexes mentioned in the Methods section that have a diverse molecular profile possessing a variety of functions and sizes.

Although experimental results play an indispensable role in validating the simulation method as we have mentioned before, the experimental determination of the contribution of the backbone hydrogen interaction is extremely difficult. Thus, the validation of the theoretical method against experimental data can only be qualitative.

We have carefully analyzed all the seven MD simulations, and we have observed 11 hydrogen bonds that were extremely stable during the whole simulation. In the 1YCR complex we observed the hydrogen bond established between the HE1 atom of the Trp23 and the O atom of the Leu54 residue of the hMDM2 protein; in the 1YCQ complex the hydrogen bond established between the HE1 atom of the Trp23 and the O atom of the Ile50 residue of the hMDM2 protein; in the 1F47 the ionic hydrogen bond established between the NH group of the Leu373 and the carboxylate group of the Asp303 residue of the binding partner and the ionic hydrogen bond between the carboxylate group of the Met248 of the ZipA protein and Leu372 of the binding partner; in the 1FCC complex the ionic hydrogen bond established between the NH group of the Ile253 and Ser254 and the carboxylate group of the Glu27 residue of the binding

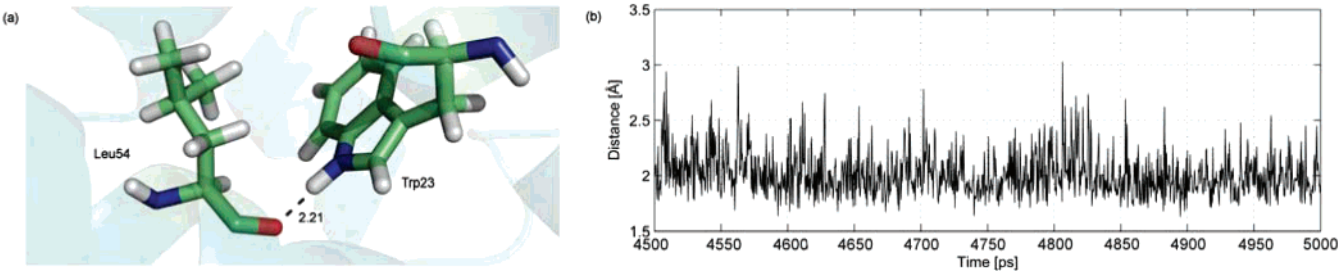

Figure 4. (a) Molecular representation of the hydrogen bond established between the HE1 atom of the Trp23 and the O atom of the Leu54 residue of the hMDM2 protein (snapshot of the production MD simulation) and (b) distance between the HE1 atom of the Trp23 and the O atom of the Leu54 residue of hMDM2 as a function of the production MD simulation time.

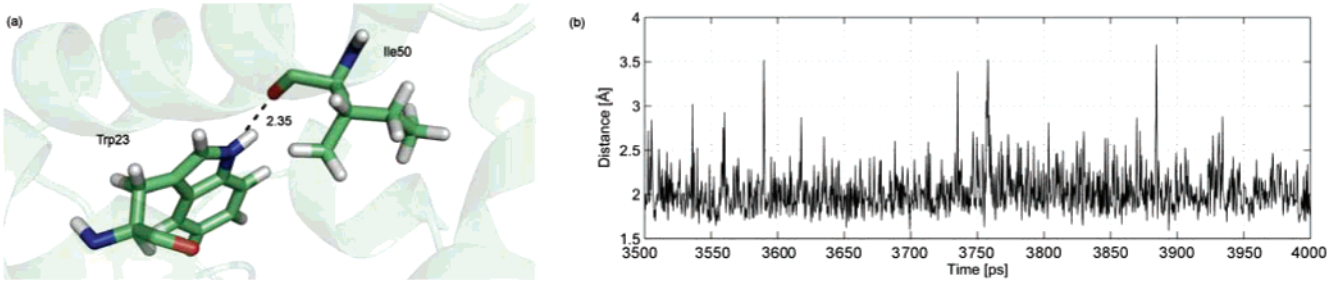

Figure 5. (a) Molecular representation of the hydrogen bond established between the HE1 atom of the Trp23 and the O atom of the Ile50 residue of the xMDM2 protein (snapshot of the production MD simulation) and (b) distance between the HE1 atom of the Trp23 and the O atom of the Ile50 residue of xMDM2 as a function of the production MD simulation time.

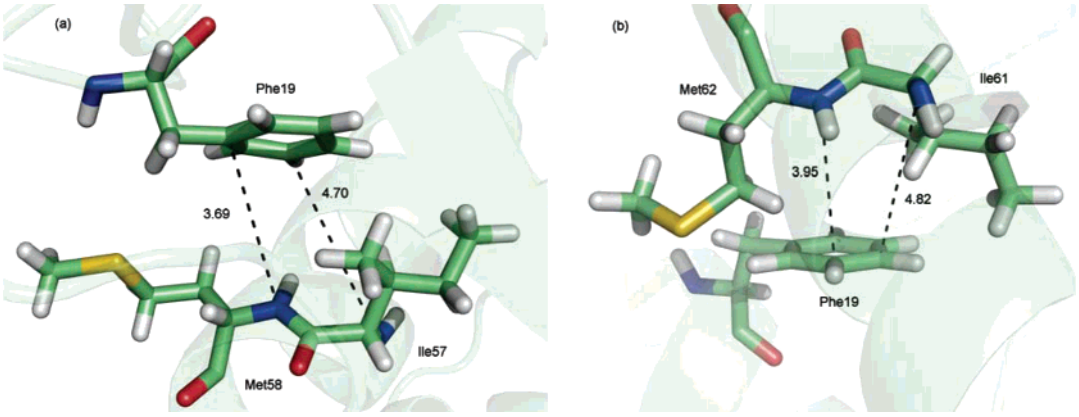

Figure 6. Molecular representation of the NH-π hydrogen bonds established between the phenyl ring of Phe19 and (a) Ile57 and Met58 of the hMDM2 protein and (b) Ile61 and Met62 of the xMDM2 protein. Figures were made from snapshots of the production MD simulation.

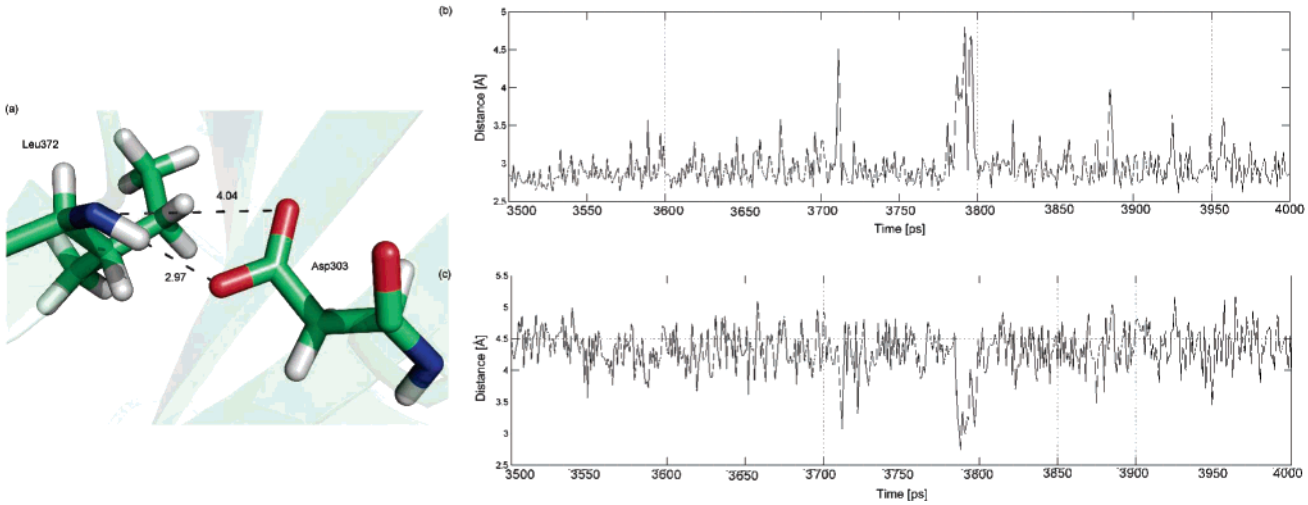

Figure 7. (a) Molecular representation of the hydrogen bond established between the N atom of the Leu373 and the O atom of the Asp303 residue of the binding partner (snapshot of the production MD simulation). (b) Distance between the N atom of Leu373 and the OD1 atom of the O atom of Asp303. (c) Distance between the N atom of Leu373 and the OD2 atom of the O atom of Asp303 as a function of the last 500 ps MD simulation time.

partner; and in the 1VFB the ionic hydrogen bond between the NH group of the Ser24 and the carboxylate group of the Asp100 residue of the binding partner. We have also observed stables NH-π hydrogen bonds established between the phenyl ring of Phe19 and Ile57 and Met58 of the hMDM2 protein as well as between the phenyl ring of Phe19 and Ile61 and Met62 of the xMDM2 protein.

By observation of Table 1 we can conclude that all the stable hydrogen bonds were detected with our computational approach with one exception only: the ionic hydrogen bond between the carboxylate group of the Met248 of the ZipA protein and Leu372 of the binding partner. In Figure 3 it is illustrated in this interaction, and as we can observe both the carboxylate and the amino group of Leu372 are close to the carboxylate group of the Met248. This fact has probably led to a repulsive interaction which justifies the nondetection by the computational approach.

A structural justification was found for every relevant energetic value obtained and shown in Table 1. An excellent correlation between the quantitative calculated free binding energy contribution of the CO and NH backbone groups of the interfacial residues and the qualitative values expected for the corresponding type of interaction was also encountered. The average $\Delta\Delta G_{\text{binding}}$ contribution of the intermolecular hydrogen bonds of the backbone is 1.77 kcal/mol, which is very similar to the average contribution of the side chain to the $\Delta\Delta G_{\text{binding}}$, with a value of 1.75 kcal/mol. If we do not consider the NH-π hydrogen bonds, then this value raises to 2.73 kcal/mol.

Complex hMDM2:P53. For the first complex we have to emphasize the contribution of the NH and CO groups of the residue Leu54, which upon charge deletion generates a $\Delta\Delta G_{\text{binding}}$ of 1.27 kcal/mol. As it can be observed in Figure 4a the HE1 atom of the hot spot Trp23 establishes a hydrogen bond with the O atom of the residue Leu54 of the hMDM2 protein. This is the only intermolecular bond established in this complex, and in Figure 4b it is plotted as the distance

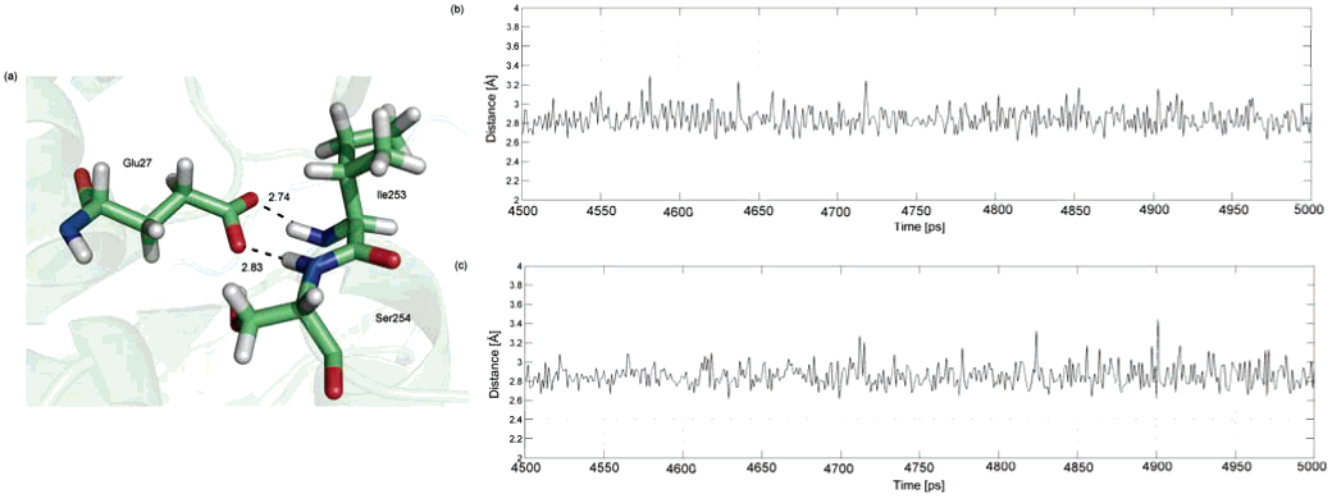

Figure 8. (a) Molecular representation of the hydrogen bond established between the NH group of the Ile253 and Ser254 and the carboxylate group of the Glu27 residue of the binding partner (snapshot of the production MD simulation). (b) Distance between the NH atom of the Ile253 residue and the OD2 atom of the carboxylate group of Glu27. (c) Distance between the NH atom of the Ser254 residue and the OD1 atom of the carboxylate group of Glu27 as a function of the last 500 ps MD simulation time.

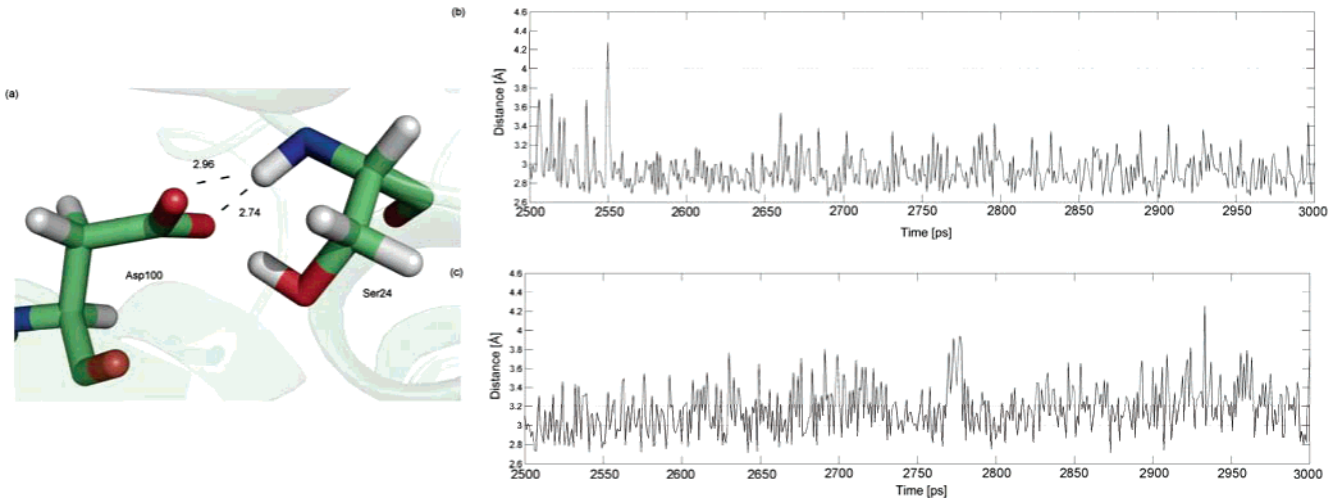

Figure 9. (a) Molecular representation of the hydrogen bond established between the N atom of the Ser24 and the carboxylate atom of the Asp100 residue of the binding partner (snapshot of the production MD simulation). (b) Distance between the N atom of Ser24 and the OD1 atom of the carboxylate group of Asp100. (c) Distance between the N atom of Ser 24 and the OD2 atom of the carboxylate group of Asp100 as a function of the last 500 ps MD simulation time.

between the two interacting atoms in function of time for the last 500 ps of the MD simulation.

Complex xMDM2:P53 and Complex hMDM2:Optimizedp53. For the complex between the P53 and xMDM2 protein (1YCQ), Ile50 is the residue that presents the highest $\Delta\Delta G_{binding}$ value (1.62 kcal/mol), because it establishes a hydrogen bond with the HE1 atom of the Trp23 residue represented in Figure 5a. This interaction is very important for complex binding with a value kept constant and under 2.0 Å during the MD simulation, as it can be perceived in Figure 5b.

We can also notice that Ile57 and Met58 present a $\Delta\Delta G_{binding}$ value of 0.36 and 0.27 kcal/mol. These values can be explained by the presence of NH-π hydrogen bonds established between those residues and the phenyl ring of Phe19 and are represented in Figure 6a. In the third complex the NH-π hydrogen bonds established between the Ile61 and Met62 residues and Phe19 with energies of 0.41 and 0.30 kcal/mol were detected (Figure 6b). When the plane formed by the amide group is roughly perpendicular to the aromatic ring and the amino group points toward the aromatic cycle, the interaction is called amino-π hydrogen bond. Even though the energetic contribution of an amino-π hydrogen bond is usually three times lower than the conventional hydrogen bond, it still contributes significantly to complex binding. It is especially important for a correct ligand orientation.[33]

Complex ZipA:FtsZ. In the fourth complex formed between a cell division protein ZipA and a cell division protein FtsZ (1F47) only a hydrogen bond was detected. It is formed between the N atom of the Leu373 and the O atom of the Asp303 residue of the binding partner and generates energy of 1.75 kcal/mol (Figure 7a). In Figure 7b,c we have plotted the distance between the N atom of Leu372 and the OD1 and OD2 atoms of the Asp303, respectively, as a

function of the last 500 ps MD simulation time. We can see by observation of Figure 7b,c that the OD1 atom has a higher contribution to the formation of a hydrogen bond as it is essentially at a 3.0 Å distance (in average 1.5 Å closer than the OD2 atom).

Complex IgG:ProteinG. For the complex formed between a human immunoglobulin IgG complexed with the C2 fragment of streptococcal protein G (1FCC) a superior absolute value of the $\Delta\Delta G_{binding}$ for the two hydrogen bonds was detected. These two bonds are formed between the OD2 group of the Glu27 residue and the NH group of the Ile253 residues and between the OD1 group of the Glu27 amino acid and the NH group of Ser254 of the C2 fragment of protein G. These bonds represented in Figure 8a generate an energy of 2.98 and 5.07 kcal/mol, respectively. By observation of Figure 8b,c we can notice that they are very stable keeping constant over the MD simulation and with an average length under 2.8 Å. The higher magnitude of the hydrogen bonds in the 1FCC complex is related to the fact that this is an ionic hydrogen bridge between two N backbone atoms and the side chain of a hot spot. In a previous work[4] we have demonstrated that alanine mutation of Glu27 generates a $\Delta\Delta G_{binding}$ of 10.27 kcal/mol. With this new computational approach, as these two hydrogen bonds produce a $\Delta\Delta G_{binding}$ of 8.05 kcal/mol we can understand the relevant interactions that make these residues so fundamental to binding in the 1FCC complex.

Complex HEL:FvD1.3. For the sixth complex formed between the lysozyme HEL and the antibody FvD1.3 (1VFB) only a hydrogen bond was detected with an energy of 3.69 kcal/mol. This bond represented in Figure 9a is formed between the N atom of Ser24 of the HEL lysozyme and the carboxylate group of the Asp100 residue of the antibody FvD1.3.

Once again the fact that the distance between the atoms is constant and less than 3.0 Å value stresses that these bonds are important for complex formation. For the complex formed between hen egg-white lysozyme (HEL) and the antibody HyHEL-10 (1C08) we have not found any hydrogen bond formation.

Conclusion

Hydrogen bonds are due primarily to partial electrostatic charges, and therefore the energetic is determined by the values of the partial charges. To understand the importance of the backbone hydrogen bonds we have measured the free binding differences generated upon deletion of the charge of the amide and carbonyl groups. To ensure electroneutrality we have distributed the remaining partial charge by the remaining atoms, which were made taking into account the proportions of the different atoms to the final charge of the amino-acid residue. This method was applied to seven structures that have a diverse molecular profile possessing a variety of functions and sizes, and a structural justification was found for every relevant energetic value obtained. An excellent correlation between the quantitative calculated free binding energy contribution of the CO and NH backbone groups of the interfacial residues and the qualitative values expected for this kind of interaction was also demonstrated.

The average $\Delta\Delta G_{binding}$ of the backbone atoms was −0.05 kcal/mol, but the average contribution of the hydrogen bonds was 1.77 kcal/mol. If we do not consider the NH-π hydrogen bonds, the average value raises to 2.73 kcal/mol. Thus, the contribution of the backbone to the $\Delta\Delta G_{binding}$ is significant. The average $\Delta\Delta G_{binding}$ contribution of the intermolecular hydrogen bonds of the backbone is very similar to the average contribution of the side chain to the $\Delta\Delta G_{binding}$, with a value of 1.75 kcal/mol.

As the backbone seems to establish really important interactions to the binding, it is not only advisable but also essential to apply this computational approach when studying a proteic complex because it clearly increases the comprehension of the protein−protein complex binding.

References

(1) Moreira, I. S.; Fernandes, P. A.; Ramos, M. J. Hot spots − a detailed review of protein-protein interface determinant amino acid residues. *Proteins* **2007**, in press.

(2) Jones, S.; Thornton, J. M. Principles of protein-protein interactions. *Proc. Natl Acad. Sci. U.S.A.* **1996**, *93*, 13.

(3) Bogan, A. A.; Thorn, K. S. Anatomy of hot spots in protein interfaces. *J. Mol. Biol.* **1998**, *280*, 1.

(4) Moreira, I. S.; Fernandes, P. A.; Ramos, M. J. Unraveling the importance of protein-protein interaction: application of a computational alanine scanning mutagenesis to the study of the IgG1: Streptococcal Protein G (C2 Fragment) complex. *J. Phys. Chem. B* **2006**, *110*, 10962.

(5) Moreira, I. S.; Fernandes, P. A.; Ramos, M. J. Hot spots computational identification- application to the complex formed between the hen egg-white lysozyme (HEL) and the antibody HyHEL-10. *Int. J. Quantum Chem.* **2007**, *107*, 299.

(6) Moreira, I. S.; Fernandes, P. A.; Ramos, M. J. Unravelling Hot Spots-a comprehensive computational mutagenesis study. *Theor. Chem. Acc.* **2007**, *117*, 99.

(7) Moreira, I. S.; Fernandes, P. A.; Ramos M. J. Computational Alanine Scanning Mutagenesis − an improved methodological approach. *J. Comput. Chem.* **2007**, *28*, 644.

(8) Xu, D.; Tsai, C. J.; Nussinov, R. Hydrogen bonds and salt bridges across protein-protein interfaces. *Protein. Eng.* **1997**, *10*, 999.

(9) Biot, C.; Buisine, E.; Kwasigroch, J. M.; Wintiens, R.; Rooman, M. Probing the energetic and structural role of amino acid/nucleobase cation-pi interactions in protein-ligand complexes. **2002**, *277*, 40816.

(10) Kumar, S.; Nussinov, R. Close-range electrostatic interactions in proteins. *Chem. Biol. Chem.* **2002**, *3*, 604.

(11) Sarkhel, S.; Desiraju, G. R. N-H..O, O-H..O, and C-H..O hydrogen bonds in protein-ligand complexes: strong and weak interactions in molecular recognition. *Proteins* **2004**, *54*, 247.

(12) Kussie, P. H.; Gorina, S.; Marechal, V.; Elenbaas, B.; Moreau, J.; Levine, A. J.; Pavletich, N. P. Structure of the MDM2 oncoprotein bound to the p53 tumor suppressor transactivation domain. *Science* **1996**, *274*, 948.

(13) Grasberger, B. L.; Schubert, C.; Koblish, H. K.; Carver, T. E.; Franks, C. F.; Zhao, S. Y.; Lu, T.; LaFrance, L. V.; Parks, D. J. Discovery and cocrystal structure of benzodiazepinedione HDM2 antagonists that activate p53 in cells. *J. Med. Chem.* **2005**, *48*, 909.

(14) Mosyak, L.; Zhang, Y.; Glasfeld, E.; Haney, S.; Stahl, M.; Seehra, J.; Somers, W. S. The bacterial cell-division protein ZipA and its interaction with an FtsZ fragment revealed by X-ray crystallography. *EMBO J.* **2002**, *19*, 3179.

(15) Sauer-Eriksson, A. E.; Kleywegt, G. J.; Uhlen, M.; Jones, T. A. Crystal structure of the C2 fragment of streptococcal protein G in complex with the Fc domain of human IgG. *Structure* **1995**, *3*, 265.

(16) Bhat, T. N.; Bentley, G. A.; Boulot, G.; Greene, M. I.; Tello, D.; Dall'Acqua, W.; Souchon, H.; Schwarz, F. P.; Mariuzza, R. A.; Poljak, R. J. Bound water molecules and conformational stabilization help mediate an antigen-antibody association. *Proc. Natl. Acad. Sci. U.S.A.* **1994**, *9*, 1089.

(17) Kondo, H.; Shiroishi, M.; Matsushimai, M.; Tsumoto, K.; Kumagai, I. Crystal structure of anti-hen egg white lysozyme antibody (HyHEL-10) Fv-antigen complex. Local structural changes in the protein antigen and water-mediated interactions of Fv-antigen and light chain-heavy chain interfaces. *J. Biol. Chem.* **1999**, *274*, 27623.

(18) Tsui, V.; Case, D. A. Theory and applications of the generalized Born solvation model in macromolecular simulations. *Biopolymers (Nucl. Acid Sci.)* **2001**, *56*, 275.

(19) Case, D. A.; Darden, T. A.; Cheatham, T. E., III; Simmerling, C. L.; Wang, J.; Duke, R. E.; Luo, R.; Merz, H. M.; Wang, B.; Pearlman, D. A.; Crowley, M.; Brozell, S.; Tsui, V.; Gohlke, H.; Mongan, J.; Hornak, V.; Cui, G.; Beroza, P.; Schafmeister, C.; Caldwell, J. W.; Ross, W. S.; Kollman, P. A. *AMBER 8*; University of California: San Francisco, CA, 2004.

(20) Cornell, W. D.; Cieplak, P.; Bayly, C. I.; Gould, I. R.; Merz, K. M., Jr.; Ferguson, D. M.; Spellmeyer, D. C.; Fox, T.; Caldwell, J. W.; Kollman, P. A. A second generation force field for the simulation of proteins, nucleic acids, and organic molecules. *J. Am. Chem. Soc*. **1995**, *117*, 5179.

(21) Ryckaert, J. P.; Ciccotti, G.; Berendsen, H. J. Numerical integration of the cartesian equations of motion of a system with constraints: molecular dynamics of n-alkanes. *J. Comput. Phys.* **1977**, *23*, 327.

(22) Pastor, R. W.; Brooks, B. R.; Szabo, A. An analysis of the accuracy of Langevin and molecular dynamics algorithms. *Mol. Phys.* **1988**, *65*, 1409.

(23) Loncharich, R. J.; Brooks, B. R.; Pastor, R. W. Langevin dynamics of peptides: The frictional dependence of isomerization rates of N-actylananyl-N′-methylamide. *Biopolymers* **1992**, *32*, 523.

(24) Izaguirre, J. A.; Catarello, D. P.; Wozniak, J. M.; Skeel, R. D. Langevin stabilization of molecular dynamics. *J. Chem. Phys.* **2001**, *114*, 2090.

(25) Rocchia, W.; Sridharan, S.; Nicholls, A.; Alexov, E.; Chiabrera, A.; Honig, B. Rapid grid-based construction of the molecular surface for both molecules and geometric objects: applications to the finite difference Poisson-Boltzmann method. *J. Comput. Chem.* **2002**, *23*, 128.

(26) Rocchia, W.; Alexov, E.; Honig, B. Extending the applicability of the nonlinear Poisson-Boltzmann equation: multiple dielectric constants and multivalent ions. *J. Phys. Chem. B* **2001**, *105*, 6507.

(27) Moreira, I. S.; Fernandes, P. A.; Ramos, M. J. Accuracy of the numerical solution of the Poisson-Boltzmann equation. *J. Mol. Struct. (Theochem*) **2005**, *729*, 11.

(28) Connolly, M. L. Analytical molecular surface calculation, *J. Appl. Crystallogr.* **1983**, *16*, 548.

(29) Massova, M.; Kollman, P. A. Computational alanine scanning to probe protein-protein interactions: a novel approach to evaluate binding free energies. *J. Am. Chem. Soc*. **1999**, *121*, 36.

CT6003824